First part

Spatially Resolved Modeling of Colicin-Induced Killing and Chemotactic Sensing in *Escherichia Coli*

Abstract

As already desribed in the general introduction, the aim of our project was to develop a synthetical killer/prey system. In this project, the chemotactic sensing in *Escherichia coli* and colicin-induced killing of a prey strain have been modeled. Colicins are special proteins produced by *E. coli* that are toxic to other bacteria. We have developed a system of partial differential equations (PDE) which could accurately describe the chemotactic sensing of the prey strain by the killer cells. Parameters were obtained from literature values. Numerous simulations with different parameters were run in order to analyse its influence on the system, especially the efficiency of the killer cells.

Contents

1 Introduction

Spatio-temporal interactions of bacterial populations is a challenging and difficult task for modeling. Bacterial strains can swim, respond to external chemicals, secrete their own signals for communication, and even produce killing factors for other bacterial species. Many of these processes are non-linear and proceed at different time and space scales.

Chemotaxis in *Escherichia coli* is one of the best studied systems of signal transduction (for recent reviews see [1, 2, 3]). In common with many other bacteria, *E. coli* can migrate towards high concentrations of attractants and avoid repellents. In the adapted state, cells perform a random walk, which becomes biased in the presence of a spatial gradient of attractant. This swimming bias is based on temporal comparisons of attractant concentrations during cell runs. If the direction of a run is favorable, i.e. up the attractant gradient or down the repellent gradient, the run becomes longer. Between two runs, the cell tumbles and reorients for the next run [4].

A number of detailed mathematical models of chemotaxis have been proposed [5, 6, 7, 8, 9, 10, 11, 12] which simulate the relations between intracellular components of the signaling network (for a recent review see [13]). However, on a long time scale, the behavior of chemotactic bacterial population can be described by (relatively) simple mechanisms in the terms of Partial Differetial Equations (for a recent review see [14]). In the PDE description, the cell densitites and the chemical concentrations are described using unknown functions of time and space variables, and their derivatives.

In this work, the spatio-temporal interactions of the killer-prey system are modeled. The killer strain is able to swim towards the prey population using the gradient of Autoinducer-2 (AI-2) secreted by the prey. In the vicinity of prey, the killer strain eliminates the prey by the Autoinducer-1-induced colicin secretion. Colicins can act in several ways. Some form pores in the inner membrane (Colicin E1), others have enzymatic activities (Colicin E9), which act as nuclease in the cytoplasm [15, 16]. Colicin-producing cells also posses an immunity protein which protects them. Yet in the case of group A colicins, on which the system and model are based on, a lysis protein is also produced causing cell lysis of the killer bacteria [16]. The signal molecules of AI-1 are secreted by the prey cells and adsorbed by the killer cells, in which they activate the production of the colicin and lysis proteins. The killer cells then lyse and release the colicin which diffuses and kills the preys in the surrounding medium.

We considered two different models shown in Figure 1. In the first model, we designed a minimal system of four non-linear reaction-diffusion PDEs to simulate the chemotactic motility of the killer population towards the prey, and the colicin killing process (Fig. 1(a) & 1(b)). To simulate the system, we approximated the original system of four PDEs by a system of 10,000 ODEs (method of lines), and solved it numerically using custom-written Matlab code. Here, AI-2 and AI-1 dynamics are modeled together by one equation (Fig. 1(a)), assuming that their secretion and diffusion rates are similar. In the second approach the two Autoinducer molecules are modeled by two separate equations (Fig. 1(b)).

2 Chemotaxis Model

The first model, in which AI-1 and AI-2 dynamics are considered simultanously, consisting of four equations: prey population (u), killer population (v), colicin concentration (c) and Autoinducer concentration (a_2). The prey cells cannot use chemotaxis, because a flagellin knock-out strain was used in the experiments. Thus the prey cell concentration can be delineated by a simple diffusion and death term caused by colicin susceptibility. Prey cells are killed by colicin at a rate which is a product of the colicin concentration (c), prey cell density (u) and the adsorption rate of colicin by prey cells (δ_u)[17].

$$\frac{\partial u}{\partial t} = D_u \Delta u - \delta_u c u. \tag{1}$$

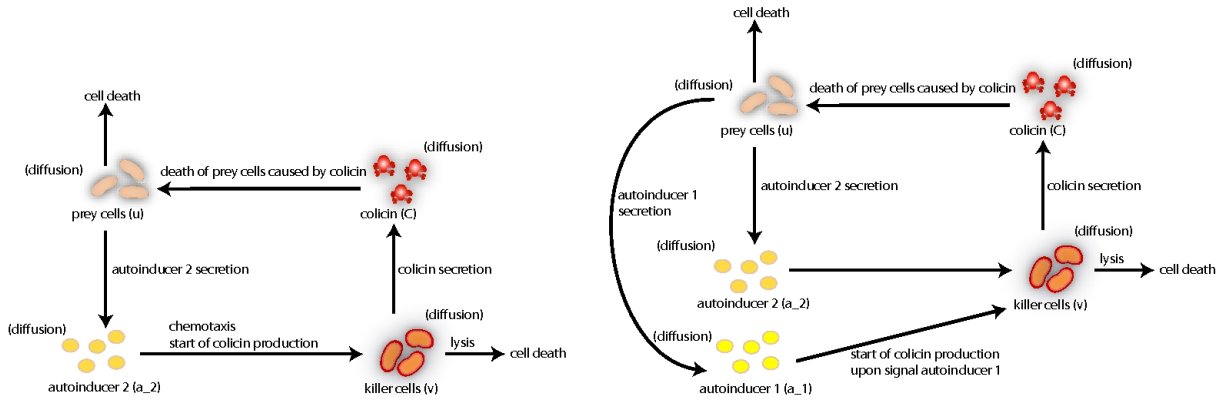

Fig. 1: Graphical representation of the modeling system. (a) In the first system AI-1 and AI-2 are modeled together in one equation. Thus AI-2 is the chemoattractant and also responsible for colicin production. **(b)**. AI-1 and AI-2 dynamics are modeled seperately which results in a more realistic model. AI-2 is only the chemoattractant, colicin production is induced by AI-1.

The killer population (v) on the other hand can diffuse and utilize chemotaxis to swim along the gradient of the chemoattractant. Furthermore, the killer cell concentration decreases due to cell lysis upon colicin secretion [17] whereas colicin production depends on the Autoinducer concentration. The chemotaxis term is based on the model by Tyson et al. [18] and on the first chemotaxis model by Keller and Segel [19].

$$\frac{\partial v}{\partial t} = D_v \Delta v - \alpha \nabla(\chi(a_2) v \nabla a_2) - \delta_v a_2 v \tag{2}$$

Parameter α reflects the chemotactic strength towards the chemoattractant. Colicin (C) and Autoinducer (a_2) dynamics are modeled with a diffusion and production term. The first approach was to use saturation kinetics for production.

$$\frac{\partial c}{\partial t} = D_c \Delta c + \beta_c \frac{v^2}{\mu_c + v^2} \tag{3}$$

$$\frac{\partial a_2}{\partial t} = D_{a_2} \Delta a_2 + \beta_{a_2} \frac{u^2}{\mu_{a_2} + u^2} \tag{4}$$

Experimentalists from our team and other results ([16][20]) suggested exponential production of colicin and Autoinducer, which is modeled as a linear term in the differential equation. The colicin concentration increases proporptional to the number of lysed cells and colicin molecules released per cell lysis [17].

$$\frac{\partial c}{\partial t} = D_c \Delta c + \beta_c \delta_v a_2 v \tag{5}$$

$$\frac{\partial a_2}{\partial t} = D_{a_2} \Delta a_2 + \beta_{a_2} u \tag{6}$$

It was also considered to add degradation terms for colicin and Autoinducer, but experimentalists from our team suggested that in the observed time span degradation can be neglected. The final

system of equations modeling AI-1 and AI-2 dynamics the same has the following structure.

$$\begin{aligned}
\frac{\partial u}{\partial t} &= D_u \Delta u - \delta_u c u \\
\frac{\partial v}{\partial t} &= D_v \Delta v - \alpha \nabla(\chi(a_2) v \nabla a_2) - \delta_v a_2 v \\
\frac{\partial c}{\partial t} &= D_c \Delta c + \beta_c \delta_v a_2 v \\
\frac{\partial a_2}{\partial t} &= D_{a_2} \Delta a_2 + \beta_{a_2} u
\end{aligned} \tag{7}$$

In this system both Autoinducer prodcution rates and diffusion constants are considered to be identical. To make it more realistic the idea was to model their dynamics seperately. Thus another equation for Autoinducer-1 was added to the system. Since both molecules are similar the basic structure looks the same. AI-1 is, like AI-2, produced by the prey cells.

$$\frac{\partial a_1}{\partial t} = D_{a_1} \Delta a_1 + \beta_{a_1} u \tag{8}$$

Besides adding another equation for AI-1 dynamics it must also be considered that colicin production is induced by AI-1, so the lysis term for the killer cells and production term for colicin need to be adopted by substitution of a_2 by a_1. Thus the final model system with different Autoinducer dynamics looks the following.

$$\begin{aligned}
\frac{\partial u}{\partial t} &= D_u \Delta u - \delta_u c u \\
\frac{\partial v}{\partial t} &= D_v \Delta v - \alpha \nabla(\chi(a_2) v \nabla a_2) - \delta_v a_1 v \\
\frac{\partial c}{\partial t} &= D_c \Delta c + \beta_c \delta_v a_1 v \\
\frac{\partial a_1}{\partial t} &= D_{a_1} \Delta a_1 + \beta_{a_1} u \\
\frac{\partial a_2}{\partial t} &= D_{a_2} \Delta a_2 + \beta_{a_2} u
\end{aligned} \tag{9}$$

$u(x,t) \in c^{2,1}\ (\Omega \times [0,T])$ describes the prey cell concentration, $v(x,t) \in c^{2,1}\ (\Omega \times [0,T])$ presents the killer cell concentration, $c(x,t) \in c^{2,1}\ (\Omega \times [0,T])$ the colicin concentration, $a_1(x,t) \in c^{2,1}\ (\Omega \times [0,T])$ Autoinducer-1 concentration and $a_2(x,t) \in c^{2,1}\ (\Omega \times [0,T])$ the chemoattractant concentration (AI-2). The $C^{2,1}$ notation stands for functions with continuous second derivative in space and first derivative in time. D_u, D_v, D_c, D_{a_1}, $D_{a_2} \in \mathbb{R}$ are diffusion coefficients for u, v, c, a_1 and a_2 respectively, and δ_u, β_{a_1}, β_{a_2}, α, β_c, $\delta_v \in \mathbb{R}$ are model parameters which can be related to experimental observations.

$$\chi(S) = \frac{\alpha K_d}{(K_d + S)^2}$$

is the sensivity function of a chemoattractant S with dissociation constant K_d.

The biological meanings of the mathematical terms on the right-hand sides of (7) and (9) are as follows.

First equation:

1. Diffusion of prey cells. Cell migration is modelled the same way as molecular diffusion, based on a random walk
2. Death of prey cells due to colicin actions

Second equation:

1. Diffusion of killer cells
2. Chemotaxis along the gradient of c towards prey cells
3. Lysis of killer cells due to colicin secretion

Third equation:

1. Diffusion of chemoattractant (AI-2)
2. Secretion of chemoattractant by prey cells

Fourth equation:

1. Diffusion of colicin
2. Secretion of colicin by prey cells

Fifth equation (only in (9)):

1. Diffusion of AI-1
2. Secretion of AI-1 by prey cells

A discussion of the parameter values will be presented in the next section. Table 1 contains a list of parameters together with meanings and suitable values.

3 Parameter estimation

The Diffusion constant of colicin is

$$D_c = 4.2 \cdot 10^{-5} \ \frac{\text{mm}^2}{\text{s}} \ [21].$$

Diffusion constants for AI-1 and AI-2 were estimated with that of aspartate as

$$D_{a_1} = D_{a_2} = 8.9 \cdot 10^{-4} \ \frac{\text{mm}^2}{\text{s}} \ [22].$$

Diffusion constants for the two bacterial populations were calculated as

$$D_u = D_v = \frac{v_{\text{cell}}^2 \cdot T_{\text{run}}}{2 \cdot (1 - 0.33)} \ [23].$$

v_{cell} is the average cell speed of 0.02 $\frac{\text{mm}}{\text{s}}$ [24]. T_{run} is the average time between two random walks with an average value of 1 s [22]. The adsorption rate of colicin by the prey population is

$$\delta_u \ = \ 6.3 \cdot \ 10^{-11} \ \frac{\text{ml}}{\text{molecule } h} = 184.2 \ \frac{\text{L}}{\text{g} \cdot \text{s}} \ [17]$$

with a molecular weight for Colicin E1 of 57,279 Da [25] which are $9.5 \cdot 10^{-20}$ g. The lysis rate for the killer population is approximately $2.28 \cdot 10^{-5} \ s^{-1}$ [17]. In our model, we need a second order rate constant, so it is further assumed that colicin production also depends on the binding of AI-1 to the cell surface. For the binding constant, the dissociation constant of aspartate ($9.44 \cdot 10^{-4} \ \frac{g}{l}$ [26]) is used. Taking lysis rate and dissociation constant into account a lysis rate of second order is achieved as

$$\delta_v = \frac{2.28 \cdot 10^{-5}}{9.44 \cdot 10^{-4}} \ \frac{\text{L}}{\text{g} \cdot \text{s}} = 0.024 \ \frac{\text{L}}{\text{g} \cdot \text{s}}$$

With each lysing killer cell about 100,000 colicin molecules are released [17]. β_C is approximated as the ratio of colicin released per cell (dry weight of 300 pg [27]). Thus

$$\beta_c = 0.032$$

For both Autoinducer molecules no production rates could be found, likely because the amount of Autoinducer produced depends on the promoter acitivity and also on external stimulus. It is assumed that the diffusion of the Autoinducer is the limiting step in its secretion, thus it should be in the same order as the diffusion coefficient. Experimental results demonstrated that about 89 % of produced Autoinducer is secreted [28]. Thus the secretion rates for AI-1 and AI-2 are estimated as

$$\beta_{a_1} = \beta_{a_2} = 0.89 \cdot 8.9 \cdot 10^{-4}\ s^{-1}$$

Table 1 summaryses all parameters with estimated values.

Table 1: Model Parameters used in the 5 equation model given with its biological meaning and suitable value.

Parameter	Biological Meaning	Value	Ref
D_u	diffusion coefficient of prey cells in [mm^2]/[s]	$3 \cdot 10^{-4}$	[22][23][24]
D_v	diffusion coefficient of killer cells in [mm^2]/[s]	$3 \cdot 10^{-4}$	[22][23][24]
D_c	diffusion coefficient of colicin in [mm^2]/[s]	$4.2 \cdot 10^{-5}$	[21]
D_{a_1}	diffusion coefficient of Autoinducer-1 in [mm^2]/[s]	$8.9 \cdot 10^{-4}$	[22]
D_{a_2}	diffusion coefficient of Autoinducer-2 in [mm^2]/[s]	$8.9 \cdot 10^{-4}$	[22]
δ_u	rate of colicin adsorption by prey cells in [l]/([g][s])	184.2	[17]
δ_v	lysis rate of killer cells combined with dissociation constant for binding of AI-1 to the cell in [l]/([g]s])	0.024	[17][26]
β_c	ratio of colicin molecules released per cell	0.032	[17][25][27]
β_{a_1}	rate of Autoinducer-1 secretion in 1/s	$0.89 \cdot 8.9 \cdot 10^{-4}$	[28]
β_{a_2}	rate of Autoinducer-2 secretion in 1/s	$0.89 \cdot 8.9 \cdot 10^{-4}$	[28]

4 Numerical Methods

In this section it is explained how a system of four or five PDEs can be solved numerically. This method is illustrated for a system which consists of four PDEs and can be extended to solve a five-equation system numerically.
To numerical integrate ODEs or PDEs the finite difference method is used:

$$\begin{aligned}
\frac{\partial u}{\partial x}(i) &\approx \frac{u(i+1)-u(i)}{h_x} \text{ (forward)} \\
\frac{\partial u}{\partial x}(i) &\approx \frac{u(i)-u(i-1)}{h_x} \text{ (backward)} \\
\frac{\partial u}{\partial x}(i) &\approx \frac{u(i+1)-u(i-1)}{2h_x} \text{ (central)}
\end{aligned}$$

The second derivative is approximated as follows.

$$\frac{\partial^2 u}{\partial x^2}(i) \approx \frac{\frac{u(i+1)-u(i)}{h_x} - \frac{u(i)-u(i-1)}{h_x}}{h_x} = \frac{u(i+1)-2u(i)+u(i-1)}{h_x^2}$$

To integrate a PDE numerically, the method of lines (MOL) [29] was used. The idea of this method is to discretize the spatial variables (Fig. 2) and then solve a system of ODEs numerically, for example with the standard routine ode45 of Matlab.

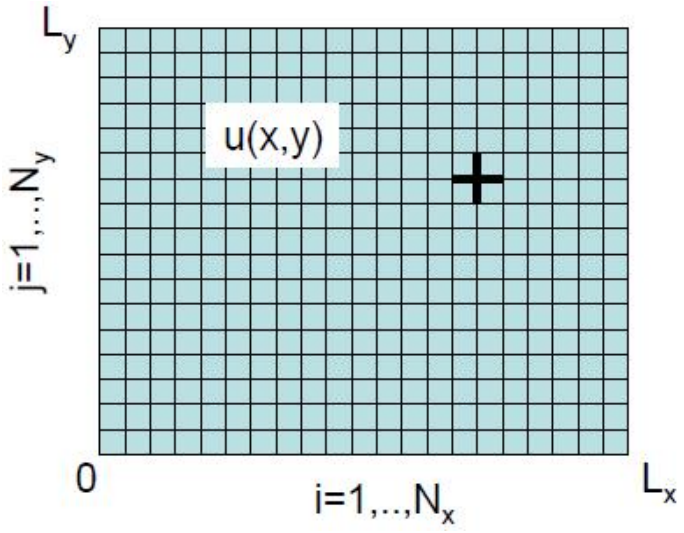

Fig. 2: Spatial Discretization of an area of $L_x \times L_y$ for width and height respectively.

Since the chemotaxis system is two dimensional, the laplace operator $\Delta z, z \in \{u, c, v, S\}$ has to be discretized for x- and y-direction, so for each equation a finite grid of finite values is obtained for x and y with height N_y and width N_x.

To use MOL it is necessary that the PDE problem be well-posed as an initial value (Cauchy) problem in at least one dimension. Therefore initial and boundary conditions need to be specified: conditions for inner points and boundary conditions for each corner and border. For the specification a conversion was done as follows:

$$u(i,j), a_2(i,j), v(i,j), c(i,j) \Rightarrow U(i), i = 1, ..., 4N_xN_y.$$

$U(1)$ corresponds to the left bottom corner, $U(4N_x)$ corresponds to the right bottom corner and $U(4N_xN_y)$ corresponds to the right top corner of the four linked grids. Furthermore a variable

$$N_{\text{row}} := 4N_x(j-1)$$

was defined which should help to address each component of the Matrix $U(i)_{i=1,...,4N_xN_y}$. This results in the following increments:
Increment by x:

$$\begin{aligned} u(i \pm 1, j) &= U(N_{\text{row}} + i \pm 1) \\ a_2(i \pm 1, j) &= U(N_{\text{row}} + i \pm 1 + N_x) \\ v(i \pm 1, j) &= U(N_{\text{row}} + i \pm 1 + 2N_x) \\ c(i \pm 1, j) &= U(N_{\text{row}} + i \pm 1 + 3N_x) \end{aligned}$$

Increment by y:

$$\begin{aligned} u(i, j \pm 1) &= U(N_{\text{row}} + i \pm 4N_x) \\ a_2(i, j \pm 1) &= U(N_{\text{row}} + i \pm 4N_x + N_x) \\ v(i, j \pm 1) &= U(N_{\text{row}} + i \pm 4N_x + 2N_x) \\ c(i, j \pm 1) &= U(N_{\text{row}} + i \pm 4N_x + 3N_x) \end{aligned}$$

For the inner points two nested for-loops were used, one for the x- and one for the y-direction to address the components of the matrix U specifying the equations of our PDE model. For the boundary

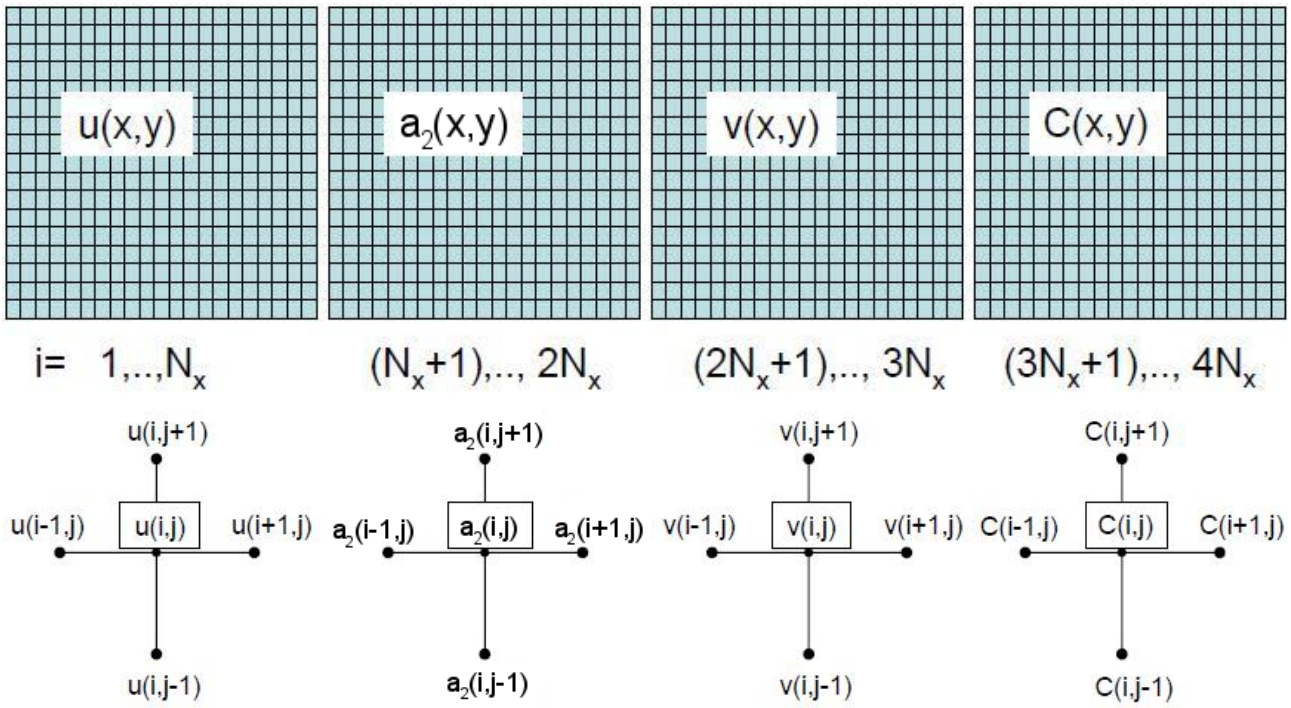

Fig. 3: Spatial discretization of a four equation system

conditions only one for-loop for the x- or the y-direction respectively was needed and for the corner points (0, 0), (0, L), (L, 0) and (L, L) the equations were specified directly.

At the four boundaries one point has only three neighbour points instead of four, so it was necessary to specify a ghost point. This was done by reflecting the conditions of the opposite point. For example a point at the boundary $x = 0$ is

$$\frac{\partial^2 z}{\partial x^2}(i) \approx \frac{2z(i+1) - 2z(i)}{h_x^2}, z \in \{u, c, v, S\}$$

The laplace operator for y does not have to be modified in this boundary and in $x = L$. In the boundaries $y = 0$ and $y = L$ the laplace operator for x does not have to be modified but $\frac{\partial^2 z}{\partial y^2}, z \in \{u, c, v, S\}$ has to be the same as for $\frac{\partial^2 z}{\partial x^2}$. In the four corners one point has only two neighbour points instead of four, so two ghost points had to be specified here the same way as was done in the boundaries.

An example shall show how the MOL method is utilized to numerically integrate the Keller-Segel PDE

$$u_t = D\Delta u - \nabla(\chi(S)u\nabla S)$$

where D is the diffusion coefficient of the cells and $\chi(S) = \frac{\alpha K_d}{(K_d+S)^2}$ is the sensitivity function of the chemoattractant S with dissociation constant K_d. The MOL approximation is

$$\frac{\mathrm{d}u_i}{\mathrm{d}t} = D\frac{u(i+1) - 2u(i) + u(i-1)}{h_x^2}$$

$$-\frac{1}{h_x}\left[0.5(\chi(i+1) + \chi(i))\frac{S(i+1) - S(i)}{h_x} - 0.5(\chi(i) + \chi(i-1))\frac{S(i) - S(i-1)}{h_x^2}\right],$$

where $\chi(i) = u(i)\frac{\alpha_s^2}{n}\frac{K_d}{(K_d+S(i))^2}$.

Regarding a system consisting of five PDEs the method is quite the same except for few changes:

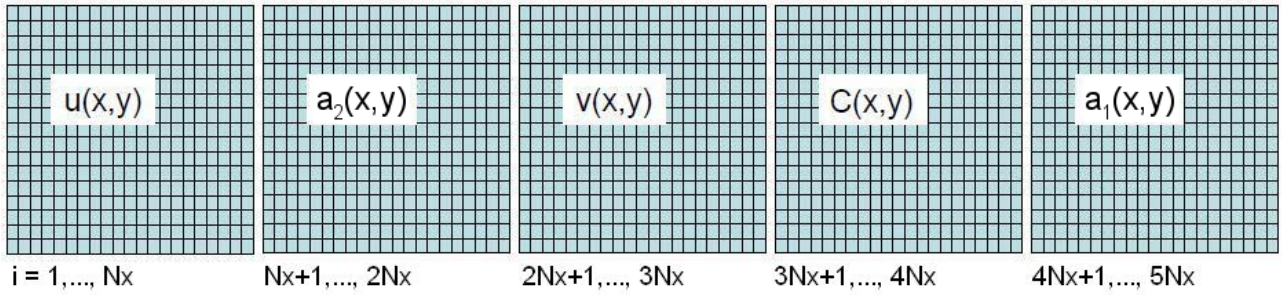

Fig. 4: Spatial discretization of the five equation system

One grid has to be added for the fifth component, the Autoinducer-1. So the conversion and the N_{nrow} variable changes to:

$$u(i,j), a_2(i,j), v(i,j), c(i,j), a_1(i,j) \Rightarrow U(i), i = 1, ..., 5N_xN_y$$

and

$$N_{\text{row}} := 5N_x(j-1).$$

$U(1)$ still corresponds to the left bottom corner, $U(5N_x)$ corresponds to the right bottom corner and $U(5N_xN_y)$ corresponds to the right top corner of the five linked grids. With these increments it is possible to address every component of the new matrix $U(i)_{i=1,...,5N_xN_y}$.
Increment by x:

$$\begin{aligned} u(i\pm1,j) &= U(N_{\text{row}}+i\pm1) \\ a_2(i\pm1,j) &= U(N_{\text{row}}+i\pm1+N_x) \\ v(i\pm1,j) &= U(N_{\text{row}}+i\pm1+2N_x) \\ c(i\pm1,j) &= U(N_{\text{row}}+i\pm1+3N_x) \\ a_1(i\pm1,j) &= U(N_{\text{row}}+i\pm1+4N_x) \end{aligned}$$

Increment by y:

$$\begin{aligned} u(i,j\pm1) &= U(N_{\text{row}}+i\pm5N_x) \\ a_2(i,j\pm1) &= U(N_{\text{row}}+i\pm5N_x+N_x) \\ v(i,j\pm1) &= U(N_{\text{row}}+i\pm5N_x+2N_x) \\ c(i,j\pm1) &= U(N_{\text{row}}+i\pm5N_x+3N_x) \\ a_1(i,j\pm1) &= U(N_{\text{row}}+i\pm5N_x+4N_x) \end{aligned}$$

For the inner points, the boundary conditions and corner points, the fifth equation just has to be added and the rest stays the same.

5 Simulation Results

Simulations were performed in Matlab® (2008a, The Mathworks, Inc.) of 2 h simulation time. Computation time was about 5-6 hours. Initial simulations were run with estimated parameters shown in Table 1 and different spatial distributions of killer and prey strains. In one set of simulations prey strains were equally distributed and killer cells set in one corner. Secondly, simulations were done with prey cells set in the center of the area and killer cells uniformly around them. In simulation movies concentration levels are encoded with different colors from white to yellow over red and finally black. White color depicts highes concentrations and black a concentration of zero with decreasing concentration inbetween. If not stated otherwise, an initial cell density of 10^9 cells/ml was used, which is typical for an *E. coli* overnight culture.

5.1 Four-PDE System

Initial simulations were run with the basic Four-PDE system. Figure 5 shows the result for placing the killer in the front corner and prey equally distributed. A more detailed focus was laid on the more

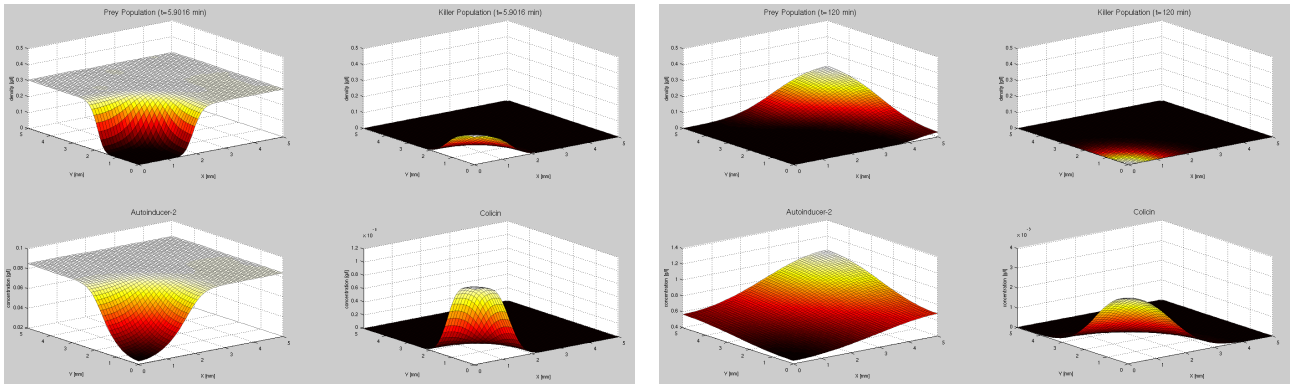

(a) (b)

Fig. 5: Simulation results for equally distributed prey and killer in corner. (a) System at about 6 min. The killer population rapidly dies due to colicin production and cell lysis. Colicin concentration is highest in the corner of about $0.6 \cdot 10^{-3}$ $\frac{\text{g}}{\text{L}}$ and diffuses over the plane. Prey cells only diffuse and die because of colicin interaction. It can be seen that after 2 h (b) little over half the prey population is dead. Parameters were used like in Table 1.

comprehensive Five-PDE system, because parameters for AI-1 and AI-2 could be varied independently. Those results are discussed in the following section.

5.2 Five-PDE System

Figure 6 shows the system where prey cells were uniformly distributed and killer cells positioned in the front left corner with initial parameters. It shows a similar outcome like for the Four-PDE system. As killer cells move out, prey density decreases. AI-1 and AI-2 gradients have the same profile as prey concentration. After two hours only about half the prey bacteria are dead. This is due to the fact that chemotactic activity of the killer cells is very low, which is a result of high AI-2 concentration. Chemotactix works best at low attractant concentration and steep gradient. This could be shown by decreasing AI-2 production to $\frac{1}{100}$ of the original value, which yielded much better swarming of the killer cells and almost complete death of prey after 2 hours (Fig. 7).

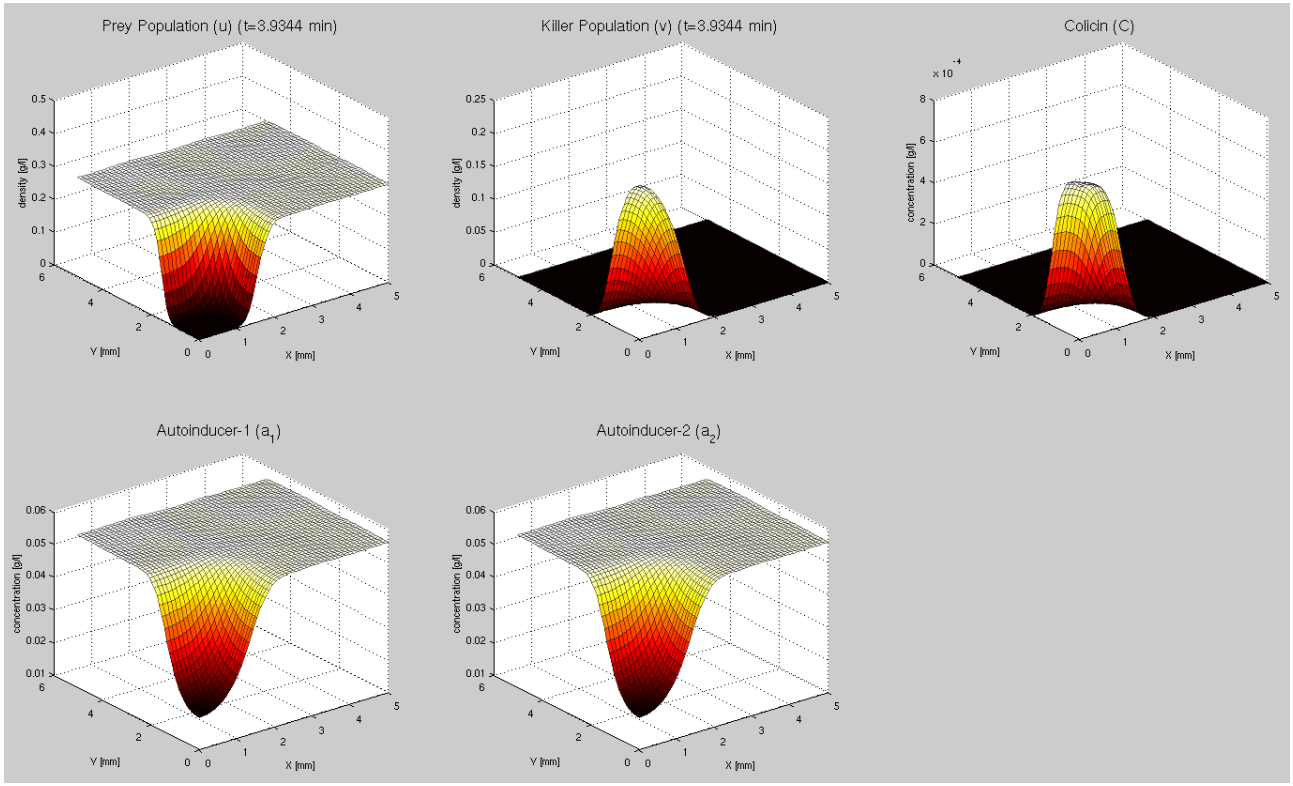

(a)

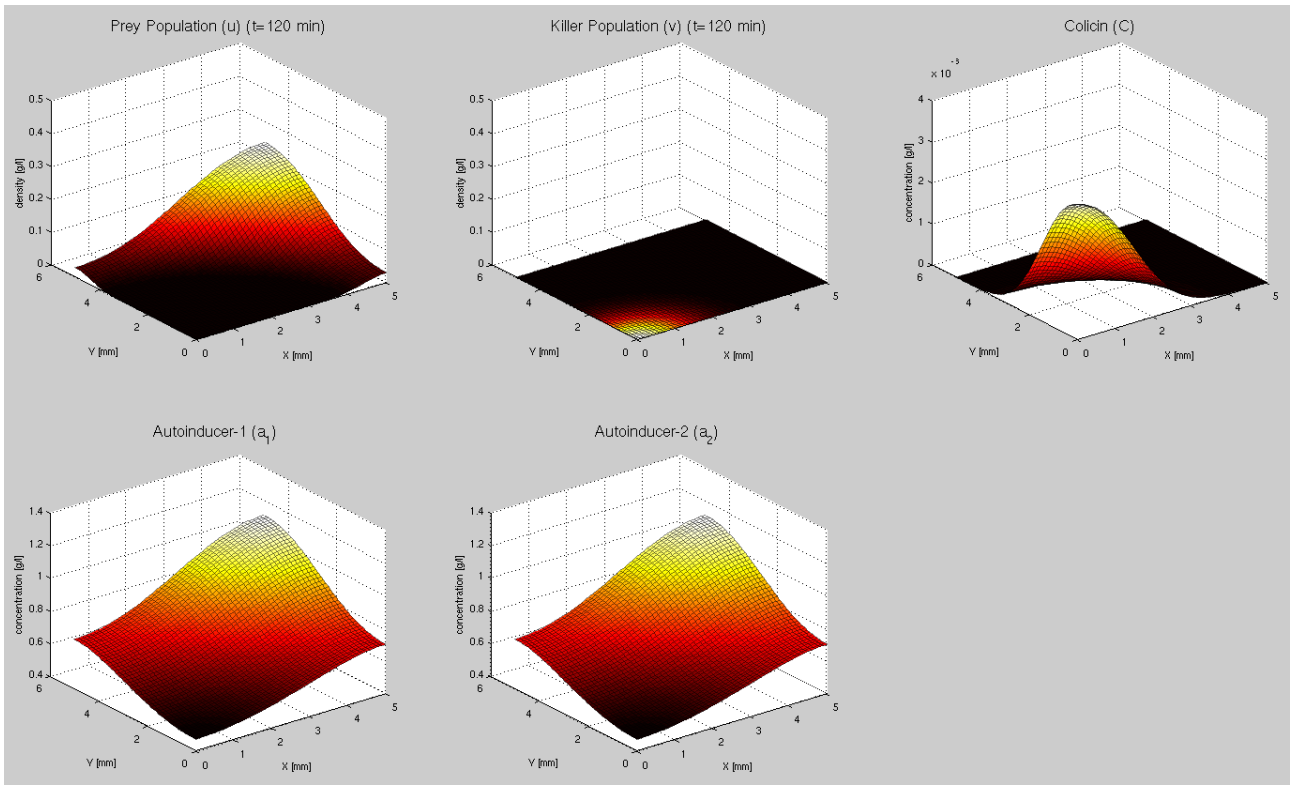

(b)

Fig. 6: Simulation results for equally distributed prey and killer in corner. (a) System at about 4 min. The killer population rapidly dies due to colicin production and cell lysis. Colicin concentration is highest in the corner of about $1 - 2 \cdot 10^{-4}$ $\frac{\text{g}}{\text{L}}$ and diffuses over the plane. Prey cells only diffuse and die because of colicin interaction. It can be seen that after 2 h (b) about half the prey population is dead. Parameters were used like in Table 1.

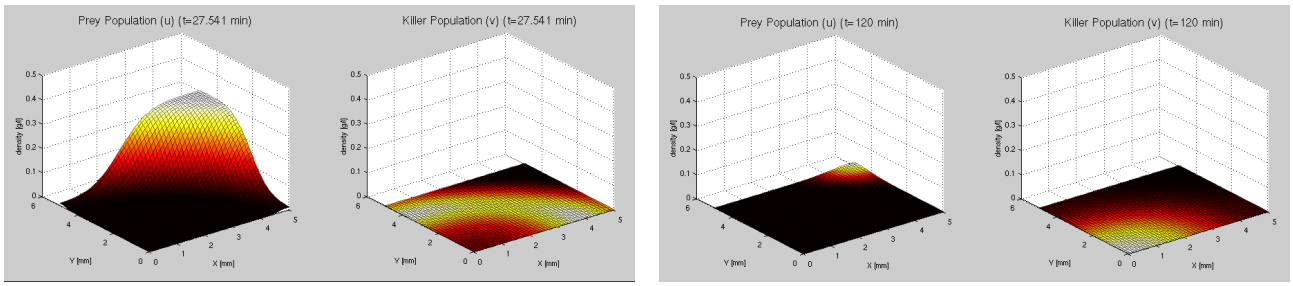

(a) (b)

Fig. 7: Simulation results with $\frac{1}{100}$ AI-2 production. Displayed are prey and killer densities. Obviously, chemotaxis activity of the killer cells is much higher, as they swarm almost over the complete area. The concentration profiles for AI-1 and AI-2 look similar to the original ones. Same applies for colicin, only that is more stretched over the plane. The further swarming of killer bacteria results in much better killing efficiency due to a larger distribution of colicin.

In real applications though it will not be possible to influence production rates of the chemoattractant. Therefore additional simulations were performed with higher chemotactic activity, reflected by the parameter α in Eq. 2, as this could be influenced experimentally by optimizing the ligand-binding domain of the chemotaxis receptor. Doubling chemotactic attraction towards AI-2 already resulted in death of more than half of prey. Setting it to 4-fold of its initial value, yielded a quite similar outcome, as for 1/100 AI-2 production (Fig. 8).

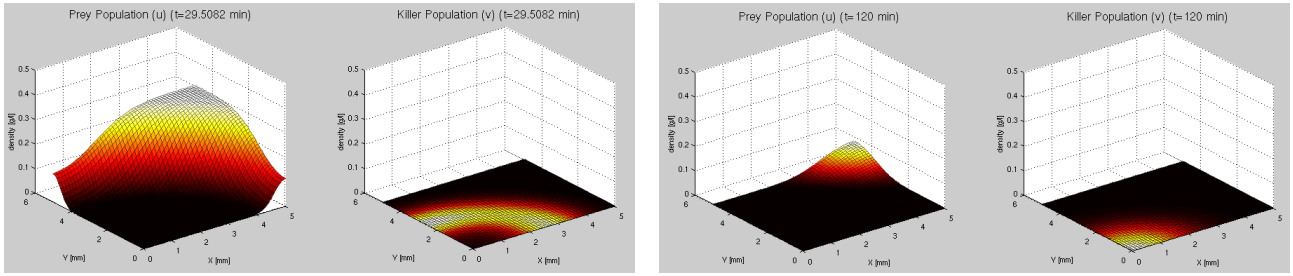

(a) (b)

Fig. 8: Simulation results with 4-fold chemotactic activity. (a) At the beginning, killer cells rapidly swarm across the plane following the AI-2 gradient. Thus colicin is much farther distributed and can kill the prey more effectively. (b) After 2 h almost all prey bacteria have been killed by predator cells, which also decrease du to cell lysis.

We were also interested how effective the sensing and killing mechanism works, if there were much less killer bacteria than prey. Ratios of 1/100 and 1/1000 of killer/prey were tested. Already with 1/100 initial cell density, no effective chemotaxis and killing could be observed. Probably there were to few cells and lysis of all killer bacteria occured too fast. It may be possible that complete death occured at some point, but then degradation of AI-1, AI-2 and colicin should be taken into account.

Besides setting the killer population in one corner with evenly distributed prey, we performed simulations with prey in the center and killer positioned around them (Fig. 9). This resulted in rapid killing of prey. Killer and colicin showed a standard 2D gaussian distribution over the whole simulation time. AI-1 and AI-2 did as well in the beginning, but equilibrated with proceeding time.

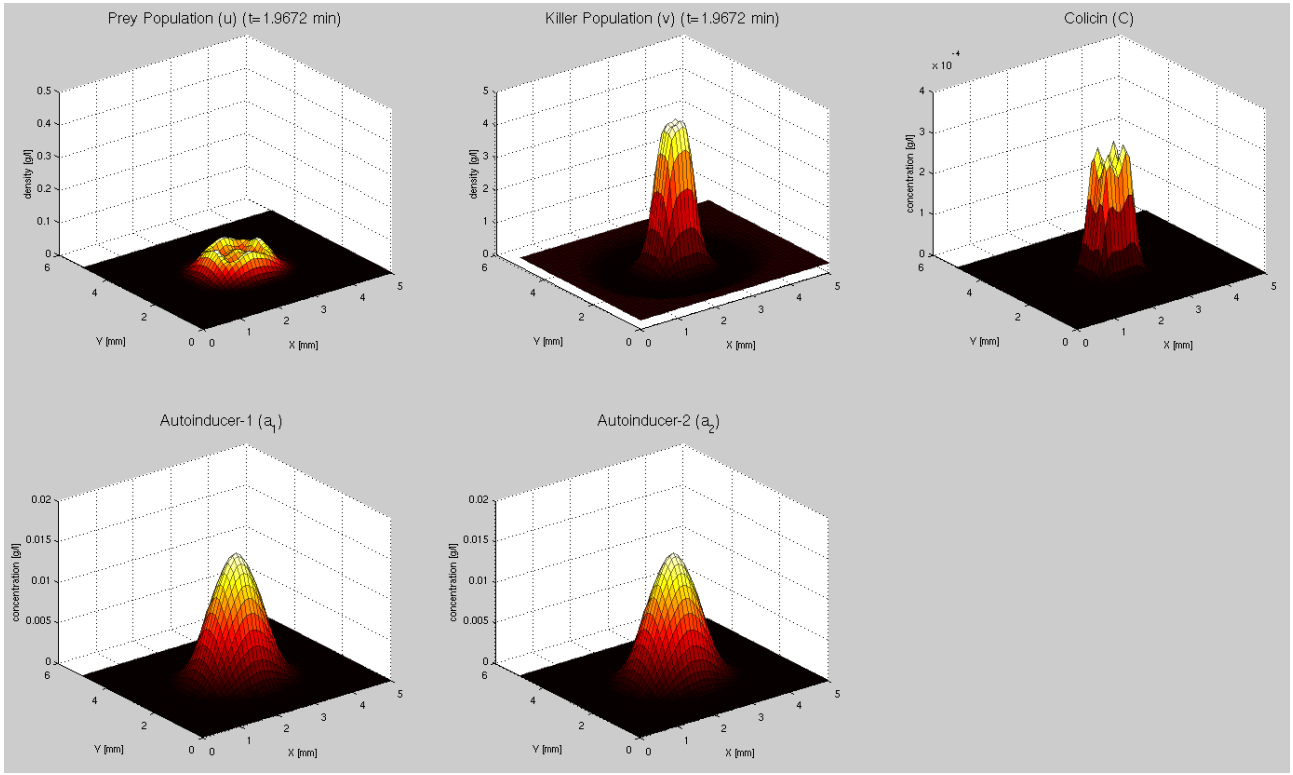

(a)

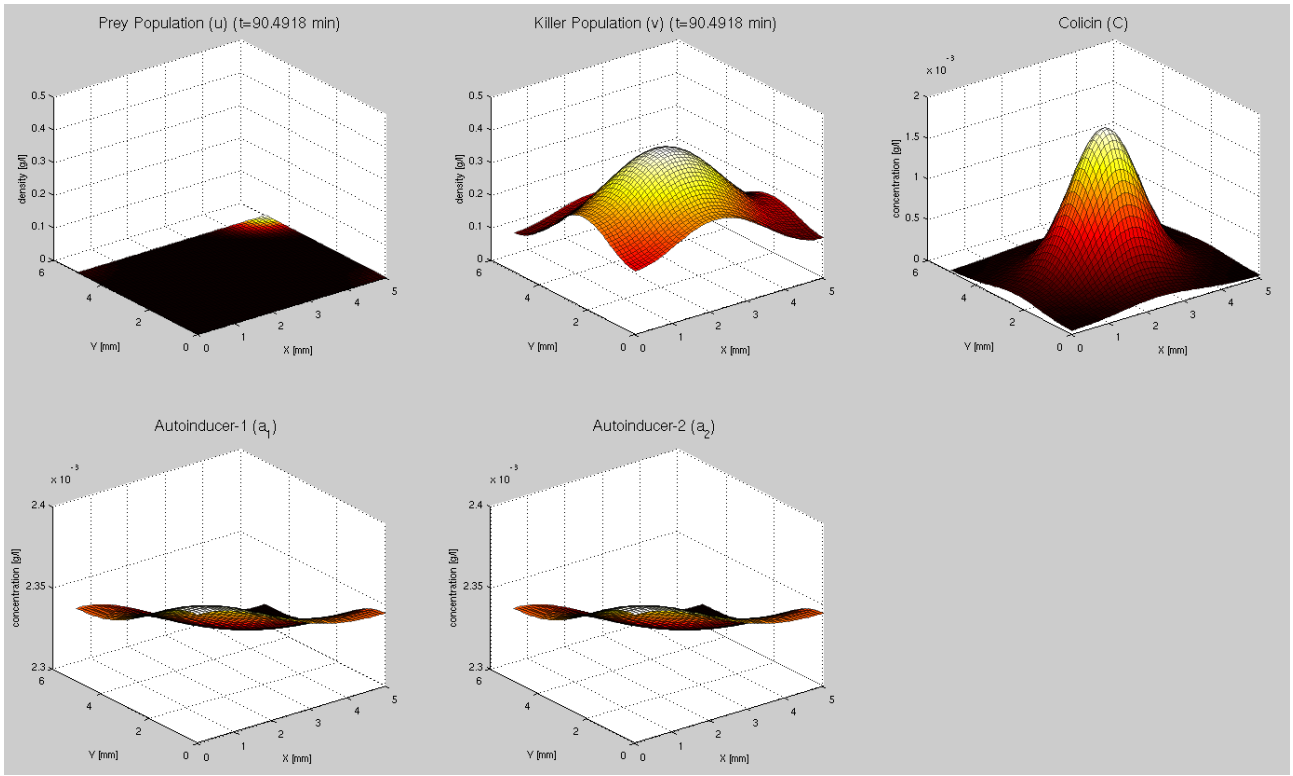

(b)

Fig. 9: Simulation results for centered prey and killer around them. Already after about 2 min (a) prey cells have diminished greatly. The prey concentration rises dramatically, but decreases afterwards due to cell lysis upon colicin production. Colicin and Autoinducer distribution looks similar to a standard gaussian distribution. Both Autoinducer diffuse outward with increasing time. After 90 min (b) nearly all prey cells are dead. Killer cells also diminish to a final concentration of about 1 g/l after 2 h (not shown).

6 Conclusions

We studied the spatio-temporal behaviour of the synthetic predator/prey system using a system of non-linear Partial Differential Equations (PDE). We have designed a minimal system consisting of four PDEs, to model the chemotactic motility of the killer cells towards the prey bacteria, and killing with colicin. Furthermore, in a more comprehensive approach, we added another PDE to simulate the dynamics of AI-1. The PDE system was numerically solved in matlab using the method of lines.

We could demonstrate that the killer strain can swim towards the prey cells using the AI-2 gradient and kill them. Most important for effective killing is the chemotactic activity towards prey. This is either accomplished by a steep attractant gradient, or high sensitivity of the chemotaxis receptor to the chemoattractant. The receptor sensitivity could possibly be altered by sequence optimization of the protein. Further we could demonstrate, that killer cells need to be present in a quite high concentration for good killing, due to lysis of the cells upon colicin production. An idea to circumvent this, is usage of a different killing mechanism, i.e. bacteriophages. This mechanism is likely to be more effective, because of the domino effect. Alternatively a different toxin could be used, to wich the killer bacteria are immune. Another reason for the fast decrease of killer cells is the rapid production of colicins. Killing could be made more effective, if colicin production is really only induced in the near vicinity of prey, which could be accomplished by usage of a signalling molecule that is either produced very slowly, with a delay compared to the chemoattractant or if it is very low diffusible.

References

[1] A. Bren, M. Eisenbach, How signals are heard during bacterial chemotaxis: protein-protein interactions in sensory signal propagation., J Bacteriol 182 (24) (2000) 6865–6873.

[2] J. J. Falke, R. B. Bass, S. L. Butler, S. A. Chervitz, M. A. Danielson, The two-component signaling pathway of bacterial chemotaxis: A molecular view of signal transduction by receptors, kinases, and adaptation enzymes, Annual Review of Cell and Developmental Biology 13 (1) (1997) 457–512.

[3] V. Sourjik, Receptor clustering and signal processing in *E. coli* chemotaxis, Trends in Microbiology 12 (12) (2004) 569–576.

[4] H. C. Berg, D. A. Brown, Chemotaxis in escherichia coli analysed by three-dimensional tracking, Nature 239 (5374) (1972) 500–504.

[5] R. G. Endres, N. S. Wingreen, Precise adaptation in bacterial chemotaxis through "assistance neighborhoods"., Proc Natl Acad Sci USA 103 (35) (2006) 13040–13044.

[6] B. W. Andrews, T.-M. Yi, P. A. Iglesias, Optimal noise filtering in the chemotactic response of escherichia coli, PLoS Computational Biology 2 (11) (2006) 1407–1418.

[7] T. S. Shimizu, S. V. Aksenov, D. Bray, A spatially extended stochastic model of the bacterial chemotaxis signalling pathway., J Mol Biol 329 (2) (2003) 291–309.

[8] B. A. Mello, Y. Tu, Quantitative modeling of sensitivity in bacterial chemotaxis: the role of coupling among different chemoreceptor species., Proc Natl Acad Sci USA 100 (14) (2003) 8223–8228.

[9] N. Barkai, S. Leibler, Robustness in simple biochemical networks., Nature 387 (6636) (1997) 913–917.

[10] D. C. Hauri, J. Ross, A model of excitation and adaptation in bacterial chemotaxis., Biophys J 68 (2) (1995) 708–722.

[11] K. Lipkow, S. S. Andrews, D. Bray, Simulated diffusion of phosphorylated chey through the cytoplasm of escherichia coli., J Bacteriol 187 (1) (2005) 45–53.

[12] P. A. Spiro, J. S. Parkinson, H. G. Othmer, A model of excitation and adaptation in bacterial chemotaxis., Proc Natl Acad Sci USA 94 (14) (1997) 7263–7268.

[13] M. Tindall, S. Porter, P. Maini, G. Gaglia, J. Armitage, Overview of mathematical approaches used to model bacterial chemotaxis i: The single cell., Bull Math Biol.

[14] M. Tindall, P. Maini, S. Porter, J. Armitage, Overview of mathematical approaches used to model bacterial chemotaxis ii: Bacterial populations., Bull Math Biol.

[15] P. D. Cotter, C. Hill, R. P. Ross, Bacteriocins: developing innate immunity for food, Nature Reviews 3 (2005) 777–788.

[16] E. Cascales, S. K. Buchanan, D. Duche, C. Kleanthous, R. Lloubes, K. Postle, M. Riley, S. Slatin, D. Cavard, Colicin biology, Microbiology and Molecular Biology Reviews 71 (1) (2007) 158–229.

[17] D. M. Gordon, M. A. Riley, A theoretical and empirical investigation of the invasion dynamics of colicinogeny, Microbiology 145 (1999) 655–661.

[18] R. Tyson, S. R. Lubkin, J. D. Murray, Model and analysis of chemotactic bacterial patterns in a liquid medium, Journal of Mathematical Biology 38 (1999) 359–375.

[19] E. Keller, L. Segel, Model for chemotaxis, Journal of Theoretical Biology 30 (1970) 225–234.

[20] M. P. DeLisa, J. J. Valdes, W. E. Bentley, Mapping stress-induced changes in autoinducer ai-2 production in chemostat-cultivated *Escherichia coli* k-12, Journal of Bacteriology 183 (9) (2001) 2918–2928.

[21] S. A. Schwartz, D. R. Helinski, Purification and characterization of colicin e1, Journal of Biological Chemistry 246 (20) (1971) 6318–6327.

[22] H. C. Berg, D. A. Brown, Chemotaxis in *Escherichia coli* analysed by three-dimensional tracking, Nature 239 (5374) (1972) 500–504.

[23] H. C. Berg, Random Walks in Biology, Princeton University Press, 1983.

[24] J. F. Staropoli, U. Alon, Computerized analysis of chemotaxis at different stages of bacterial growth, Biophysics Journal 78 (2000) 513–519.

[25] M. Yamada, Y. Ebina, T. Miyata, T. Nakazawa, A. Nakazawa, Nucleotide sequence of the structural gene for colicin e1 and predicted structure of the protein, Proc Natl Acad Sci USA 79 (1982) 2827–2831.

[26] V. Sourjik, H. Berg, Receptor sensitivity in bacterial chemotaxis, Proc Natl Acad Sci USA 99 (1) (2002) 123–127.

[27] *E. coli* statistics.
URL `http://redpoll.pharmacy.ualberta.ca/CCDB/cgi-bin/STAT_NEW.cgi`

[28] H. B. Kaplan, E. P. Greenberg, Diffusion of autoinducer is involved in regulation of the *Vibrio fischeri* luminescence system, Journal of Bacteriology 163 (3) (1985) 1210–1214.

[29] W. E. Schiesser, The numerical method of lines, Academic Press, 1991.